

Theory of electronic, vibrational, and superconducting properties of fcc silicon

Amy Y. Liu, K. J. Chang,* and Marvin L. Cohen

Department of Physics, University of California, Berkeley, California 94720
and Materials and Chemical Sciences Division, Lawrence Berkeley Laboratory, Berkeley, California 94720
 (Received 21 September 1987)

We present a theoretical calculation of the properties of the fcc, high-pressure structural phase of Si. The electronic and phonon properties have been studied and we predict the system to be a free-electron-like metal with a very stiff lattice. In addition, we estimate the superconducting transition temperature to be approximately 2 K based on calculations of the electron-phonon coupling constant λ . Comparisons are made with the results of previous calculations for Al.

I. INTRODUCTION

In recent years, the high-pressure behavior of silicon has been studied extensively both experimentally¹⁻³ and theoretically.⁴⁻⁶ Silicon undergoes a series of structural phase transitions with pressure: cubic diamond (CD) to β -Sn, to simple hexagonal, to hexagonal close packed, to face-centered cubic. These transitions are observed at pressures of approximately 10.6 (CD $\rightarrow\beta$ -Sn),^{1,2} 14.8 (β -Sn \rightarrow sh),² 38.5 (sh \rightarrow hcp),^{1,2} and 78.0 (hcp \rightarrow fcc) GPa.³ The existence of hcp and fcc silicon was anticipated theoretically⁵ and the theoretical calculations have been successful in reproducing the observed sequence of pressure induced phase transitions. In addition, the electronic, vibrational and superconducting properties of the lowest three compressed phases have been investigated. All the compressed phases have been found to be metallic, and in fact, theory successfully predicted^{6,7} that the hexagonal phases would be superconducting with transition temperatures in the range of 3-9 K. The β -Sn phase had been observed to be superconducting earlier.⁸

The calculations in this work are based on an *ab initio* pseudopotential total energy scheme.⁹ The results of previous studies⁵ using this method to investigate the pressure-induced structural phase transitions in Si are shown in Fig. 1. The calculated total energies of Si in different crystal structures as a function of volume is fit to Murnaghan's equation of state¹⁰ and plotted. Since the CD phase has the lowest minimum total energy, it is the most stable phase of silicon at ambient pressures. As pressure is applied, the volume decreases, and the transition to the β -Sn phase occurs along the common tangent line between the CD and β -Sn curves. The transition pressure is the negative of the slope of the tangent line. This method yields transition pressures and volumes to within 10% of the measured results for the CD $\rightarrow\beta$ -Sn, β -Sn \rightarrow sh, and sh \rightarrow hcp transitions. For the transition from hcp to fcc, there is a somewhat larger discrepancy between experiment and theory for the transition pressure. While experimental results find that the transition occurs at 78 GPa, theory predicts a transition pressure of 116 GPa. Transition volumes agree, however, to within a few percent.

In this paper, we present the results of theoretical calculations of the properties of Si in the fcc phase. In the following sections, we first give a description of the calculational methods used in this study (Sec. II). In Sec. III, the results of the calculations for the electronic and phonon properties are presented. In addition, we discuss the electron-phonon interaction and superconductivity in fcc Si. The system is predicted to be a free-electron-like metal which becomes superconducting around 2 K. Finally, some concluding remarks are made in Sec. IV.

II. CALCULATIONAL METHODS

Since the calculational methods used are described elsewhere, we include only a brief discussion here. The method used is based on an *ab initio* pseudopotential total energy approach,⁹ where the Si pseudopotential is generated using the atomic number as input. The structural and electronic properties can then be computed directly within the local density functional approxima-

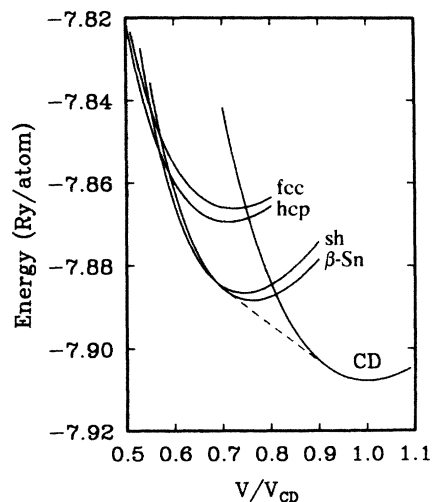


FIG. 1. Calculated total energy as a function of volume for Si in various crystal structures. The volumes are normalized to V_{CD} , the calculated equilibrium volume in the cubic-diamond phase. The dashed line indicates the path of the pressure-induced transition from the diamond to the β -Sn phase.

tion. The pseudopotential used was previously tested and found to be successful in predicting the ground-state properties of Si.⁴ The vibrational spectrum and the electron-phonon coupling are evaluated with the frozen phonon method used in conjunction with supercells.¹¹ For all of these calculations, the only input needed is atomic information, i.e., atomic mass and atomic number.

The superconducting transition temperature is calculated from the McMillan equation.¹² The parameter λ appearing in that equation is the Brillouin zone average of the wave-vector-dependent electron-phonon coupling parameter, $\lambda_{\mathbf{q}}$, which in turn is the sum of the branch-dependent parameter, $\lambda_{\mathbf{q}\nu}$, over all phonon branches ν . The function $\lambda_{\mathbf{q}\nu}$ is related to the Fermi surface average of the electron-phonon matrix element as follows:

$$\lambda_{\mathbf{q}\nu} = 2N(0) \frac{\langle\langle |g(n\mathbf{k}, n'\mathbf{k}', \mathbf{q}\nu)|^2 \rangle\rangle}{\hbar\omega_{\mathbf{q}\nu}} \quad (1)$$

where $N(0)$ is the electron density of states at the Fermi level, $\omega_{\mathbf{q}\nu}$ is the phonon frequency corresponding to the wave vector \mathbf{q} and branch ν , and $\langle\langle |g|^2 \rangle\rangle$ denotes a Fermi surface average of g . The standard definition of the square of the electron-phonon matrix element is

$$|g(n\mathbf{k}, n'\mathbf{k}', \mathbf{q}\nu)|^2 = \frac{\hbar\Omega_{\text{BZ}}}{2M\omega_{\mathbf{q}\nu}} \left| \left\langle \psi_{n\mathbf{k}}^0 \left| \hat{\epsilon}_{\mathbf{q}\nu} \cdot \frac{\delta V}{\delta \mathbf{R}} \right| \psi_{n'\mathbf{k}'}^0 \right\rangle \right|^2 \delta(\mathbf{k} - \mathbf{k}' - \mathbf{q}), \quad (2)$$

where M is the atomic mass, Ω_{BZ} is the volume of the Brillouin zone, $\hat{\epsilon}_{\mathbf{q}\nu}$ is the phonon polarization vector, $\psi_{n\mathbf{k}}^0$ is the Bloch wave function of the state \mathbf{k} in band n for the undistorted crystal, and $\delta V/\delta \mathbf{R}$ is the self-consistent change in the crystal potential caused by the phonon distortion. We note that the function $\lambda_{\mathbf{q}\nu}$ can be related to the phonon linewidth, $\gamma_{\mathbf{q}\nu}$, since

$$\gamma_{\mathbf{q}\nu} = 2\pi\omega_{\mathbf{q}\nu} \langle\langle |g|^2 \rangle\rangle N^2(0). \quad (3)$$

In our calculations the crystal potentials, total energies, and electronic wave functions are computed self-consistently both for the perfect crystal and for the crystal distorted by a frozen phonon. The atoms in the distorted lattice are positioned according to

$$\mathbf{R}_l = \mathbf{R}_l^0 + \mathbf{u}_{\mathbf{q}\nu} \sin(\mathbf{q} \cdot \mathbf{R}_l^0), \quad (4)$$

where \mathbf{R}_l^0 is the equilibrium atomic position and $\mathbf{u}_{\mathbf{q}\nu}$ is the phonon displacement vector. Typically, the amplitude of the displacement vector is chosen to be a few percent of the lattice constant.

Phonon frequencies are extracted from the difference in total energy of the distorted and undistorted lattices. The change of potential caused by phonon distortion which appears in the expression for $|g|^2$ is replaced by

$$\frac{\delta V}{\delta \mathbf{R}} = \frac{V_{\mathbf{q}\nu} - V_0}{\bar{u}_{\mathbf{q}\nu}} \quad (5)$$

where V_0 and $V_{\mathbf{q}\nu}$ are the self-consistent potentials calcu-

lated for the undistorted and distorted crystals, and $\bar{u}_{\mathbf{q}\nu}$ is the root-mean-square phonon amplitude. We use supercells where the phonon wave vector is commensurate with the original undistorted lattice, i.e., $n\mathbf{q} = \mathbf{G}$, where \mathbf{G} is a reciprocal-lattice vector of the undistorted lattice. This maps the state $\mathbf{k}' + \mathbf{q}$ back to \mathbf{k} , and thus eliminates the δ function in Eq. (2). Gaussian broadening of the δ functions involved in the Fermi surface averaging of g is employed to ensure good numerical convergence.

In the present calculations we have computed contributions to λ from three directions: [100], [110], and [111]. In particular, the wave vectors used are $\mathbf{q} = (2\pi/a)(1, 0, 0)\alpha$, $(2\pi/a)(1, 1, 0)\alpha$, and $(\pi/a)(1, 1, 1)\alpha$, with $\alpha = 1, \frac{2}{3}, \frac{1}{2}, \frac{1}{3}$. The corresponding supercells contain 2, 3, 4, and 6 atoms, respectively. The Brillouin zone average of λ is obtained by performing a spherical average along each of the three calculated directions and then taking the average of the results, with the symmetry of each direction taken into account.

III. RESULTS AND DISCUSSION

All of our calculations are done on Si in the fcc structure at the transition volume and pressure predicted by Chang and Cohen.⁵ This corresponds to a lattice constant of 3.32 Å and a volume of 62% of the equilibrium fcc volume, i.e., 62% of the volume at which the minimum occurs on the total energy curve for the fcc structure. Although the calculated transition pressure is considerably higher than that found in experiment, the calculated transition volume agrees well. At this point, we are not able to explain this discrepancy.

The calculations of the electronic properties of fcc Si indicate that the system is highly free-electron-like. The band structure and density of states are illustrated in Fig. 2. The Fermi level lies at 19.45 eV. The density of states was calculated using the tetrahedron method, and Fig. 2 shows that it follows the free-electron model very closely. The value of the density of states at the Fermi energy is calculated to be 4.0 states $\text{Ry}^{-1} \text{atom}^{-1}$, while the free-electron model yields 3.9 states $\text{Ry}^{-1} \text{atom}^{-1}$.

The valence charge density in the (100) plane is plotted in Fig. 3. It is useful to compare this to the charge density in other fcc metals. In particular, the fcc Si charge density looks qualitatively similar to that of Al.¹³ Since Al exhibits free-electron-like behavior, the similarity of charge densities provides more evidence for the free-electron character of fcc Si.

It is interesting to examine how the electronic properties of Si change as it undergoes the series of pressure-induced transitions. In the CD phase, Si has strong covalent bonds. As pressure is applied, the covalent bonds coexist with metallic bonding in the β -Sn and sh phases. Finally, in the most highly compressed phase (fcc), all the covalent character is suppressed, resulting in a free-electron metal. It is striking to compare the structurally similar CD and fcc phases, since one is the textbook example of covalent bonding while the other exhibits free-electronlike metallic bonding. This illustrates how pressure can destroy strong s - p^3 covalent bonding and force bond charge into interstitial sites resulting in metallic character.

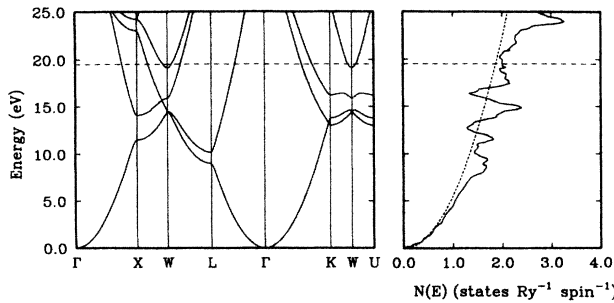


FIG. 2. Calculated band structure and density of states for fcc Si. The Fermi level is indicated by the horizontal dashed line. The dotted curve marks the free-electron density of states ($\sim E^{1/2}$).

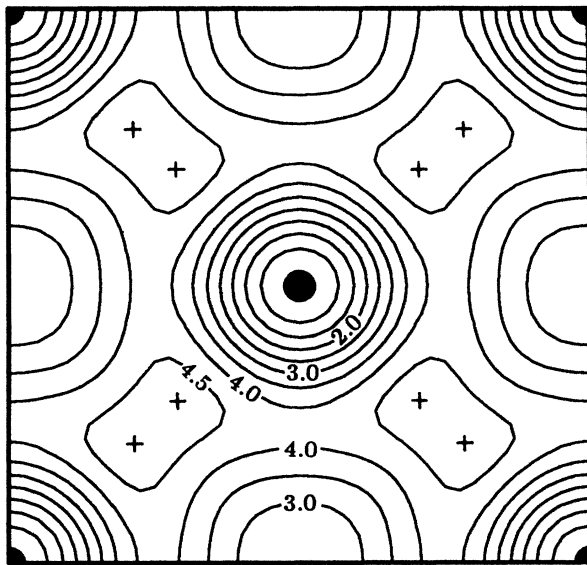


FIG. 3. Calculated valence charge density of fcc Si in the (100) plane. The units are in electrons per unit cell, hence 4.0 is the average density. The contour step is 0.5 electrons per unit cell. The crosses mark the locations where the charge density reaches its maximum value of 4.76 electrons per unit cell.

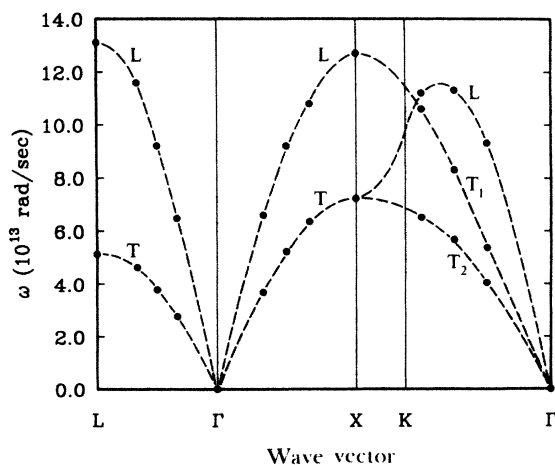


FIG. 4. Phonon frequencies as a function of q . The dashed lines are drawn through the calculated points to guide the eye.

The calculated phonon spectrum in the [100], [111], and [110] directions is displayed in Fig. 4. Comparison with the spectrum of Al (Ref. 14) reveals that the dispersion curves are very similar in shape, but that the Si frequencies are higher than those of Al by a factor of 2. The large frequencies found in Si can be explained by the fact that we are considering a highly compressed state with a volume of 62% of the equilibrium fcc volume. If Si were stable in the fcc structure at the equilibrium volume, we would expect the frequencies to be close to those of Al because the two systems have comparable atomic masses and similar electronic structure. Compression, however, stiffens the Si lattice and thus leads to the higher-energy phonon spectrum.

The large phonon frequencies result in a large velocity of sound. The longitudinal velocity of sound is estimated to be 10^6 cm/sec. The bulk modulus, which can be calculated both from the velocity of sound and from Murnaghan's equation of state, is found to be 5.0×10^2 GPa. For comparison, the material with the largest bulk modulus at ambient pressures is carbon in the diamond phase. Its bulk modulus is 5.5×10^2 GPa.

The calculated values of the wave vector dependent electron-phonon coupling constants are tabulated in Table I, and the phonon linewidths are plotted in Fig. 5. The behavior of λ_{qv} in each of the three directions is similar, justifying to some extent our spherical averaging procedure. The decreasing behavior of λ_{qv} as a function of q can be explained by examining Eq. (1) within the free electron model. In that case, the electron-phonon matrix element is a function of (q, ν) only, and its Fermi surface average can be factorized as follows:

$$\langle\langle |g|^2 \rangle\rangle = |g(q, \nu)|^2 \langle\langle \Omega_{BZ} \delta(\mathbf{k} - \mathbf{k}' - \mathbf{q}) \rangle\rangle. \quad (6)$$

The first term gives the strength of the matrix element, while the second measures the degree of Fermi surface nesting. Within the free-electron model with a spherical Fermi surface and Thomas-Fermi screening, $|g|^2$ is proportional to q^2/ω_{qv} for small q , and the nesting

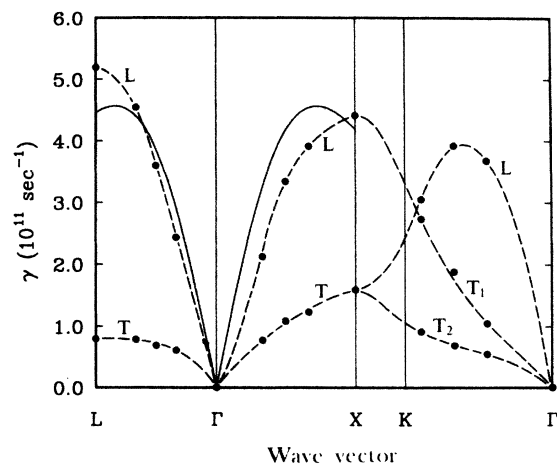


FIG. 5. Phonon linewidth as a function of q . The solid lines indicate the results from the free-electron model using a spherical Fermi surface and Thomas-Fermi screening. The dashed lines are drawn through the calculated points to guide the eye.

TABLE I. Calculated values of λ_{qv} and λ_q . The two transverse modes are degenerate in the [100] and [111] directions. The polarization vectors for the nondegenerate transverse modes in the [110] direction at $\hat{\epsilon}_{T_1}=(0,0,1)$ and $\hat{\epsilon}_{T_2}=(1,-1,0)/\sqrt{2}$.

α	λ_L	λ_{T_1}	λ_{T_2}	λ_q
[100] direction				
$\frac{1}{3}$	0.16	0.19		0.54
$\frac{1}{2}$	0.13	0.13		0.39
$\frac{2}{3}$	0.11	0.10		0.31
1 (X)	0.09	0.10		0.29
[111] direction				
$\frac{1}{3}$	0.19	0.26		0.71
$\frac{1}{2}$	0.14	0.16		0.46
$\frac{2}{3}$	0.11	0.12		0.35
1 (L)	0.10	0.10		0.30
[110] direction				
$\frac{1}{3}$	0.14	0.12	0.11	0.37
$\frac{1}{2}$	0.10	0.09	0.07	0.26
$\frac{2}{3}$	0.08	0.08	0.07	0.23
1 (X)	0.10	0.09	0.10	0.29

function varies as $1/q$. Therefore, from Eq. (1), $\lambda_{qv} \sim (1/\omega)(q^2/\omega)(1/q) \sim q/\omega^2$. Since $\omega \sim q$ for small q , we expect that in a free-electron-like metal, $\lambda \sim 1/q$ for small q . Figure 5 shows that the free-electron model yields phonon linewidths close to the self-consistently calculated values for the longitudinal branches in the [100] and [111] directions. Since the simple free-electron model used does not include umklapp scattering processes, it is not valid for the transverse modes.

In comparison with Al (Ref. 14), the values of λ_q for fcc Si at the zone boundaries are similar, but within the zones, λ_q is considerably smaller in Si. This is probably a result of the pressure induced stiffness of the Si lattice under consideration. After spherical averaging, however, we find $\lambda=0.31$, which is only slightly lower than the value for Al. This is because the phase-space volume weights λ towards the zone boundary values.

Our calculations indicate that fcc Si is a superconductor. In order to calculate the superconducting properties using the McMillan equation, we need, in addition to the quantities already discussed, the Debye temperature and the Coulomb interaction term μ^* . The Debye temperature is estimated by using the known value for Al scaled by the maximum longitudinal acoustic phonon frequency in the [100] direction. This yields a value of $T_D=859$ K. To estimate μ^* , we use the Bennemann-Garland empirical equation¹⁵ which gives μ^* as a function of the density of states. This relation scales μ^* with the renormalized density of states, $N/(1+N)$. Scaling from the density of states of Al and using the μ^* which produces the ob-

served T_c in Al, we find that $\mu^* \approx 0.06$ for our system. The McMillan equation then yields a transition temperature of 2.0 K.

Since the transition temperature depends exponentially on λ and μ^* , T_c is very sensitive to small changes in either of these parameters. The dominant dependence, however, is through $\lambda - \mu^*$, so it is sufficient to examine the sensitivity of T_c to changes in λ alone. To estimate the uncertainty in the calculated transition temperature, we vary the value of λ by $\pm 15\%$ and estimate the resulting changes in T_c . For $\lambda=0.26$, we get $T_c=0.6$ K, and for $\lambda=0.36$, we get $T_c=4.3$ K.

The calculated transition temperature of 2.0 K is comparable to that of Al (1.2 K) at ambient pressures. The stiffness of the Si fcc lattice gives a higher Debye temperature, but at the same time, lowers λ slightly. These two effects appear to cancel, giving a T_c comparable to Al. On the other hand, this T_c is somewhat lower than those found in the less compressed metallic phases of Si. For example, the sh phase is found to be superconducting with a T_c of up to 8.2 K. The lower T_c in the fcc phase can be attributed to the smaller λ in that phase, which, in turn, can be accounted for by the higher-energy phonon spectrum.

IV. CONCLUSIONS

We have done an *ab initio* pseudopotential calculation within the local density functional approximation to explore the metallic fcc phase of highly compressed Si. The calculation shows that the material exhibits free-electron-like behavior similar to Al, and therefore Si provides a good example of how the application of pressure can destroy covalent bonds. The calculated phonon spectrum has high energy modes indicating a very stiff lattice with a large bulk modulus comparable to that of diamond. The electron-phonon coupling in this system has also been studied, and we predict that the material is a superconductor with a transition temperature near 2 K.

We hope that this work leads to experimental studies on fcc Si. The necessary pressure range of 100 GPa is now attainable in diamond anvil cells. Further experimental work will serve not only to check our predictions related to superconductivity, but also to explore the normal state properties of this interesting system.

ACKNOWLEDGMENTS

We wish to thank Dr. Jose Luis Martins and Dr. Robert Dandrea for helpful discussions. Support for this work was provided by National Science Foundation Grant No. DMR-8319024 and by the Director, Office of Energy Research, Office of Basic Energy Sciences, Materials Sciences Division of the U.S. Department of Energy under Contract No. DE-AC03-76SF00098. Cray computer time at the National Magnetic Fusion Energy Computer Center was provided by the U.S. Office of Energy Research of the Department of Energy.

- *Present address: Xerox Palo Alto Research Laboratories, Palo Alto, CA 94304.
- ¹H. Olijnyk, S. K. Sikka, and W. B. Holzapfel, *Phys. Lett.* **103A**, 137 (1984).
- ²J. Z. Hu and I. L. Spain, *Solid State Commun.* **51**, 263 (1984).
- ³S. J. Duclos, Y. K. Vohra, and A. L. Ruoff, *Phys. Rev. Lett.* **58**, 775 (1987).
- ⁴M. T. Yin and M. L. Cohen, *Phys. Rev. B* **26**, 5668 (1982).
- ⁵K. J. Chang and M. L. Cohen, *Phys. Rev. B* **31**, 7819 (1985).
- ⁶M. M. Dacorogna, K. J. Chang, and M. L. Cohen, *Phys. Rev. B* **32**, 1853 (1985).
- ⁷K. J. Chang, M. M. Dacorogna, M. L. Cohen, J. M. Mignot, G. Chouteau, and G. Martinez, *Phys. Rev. Lett.* **54**, 2375 (1985).
- ⁸J. Wittig, *Z. Phys.* **195**, 215 (1966).
- ⁹M. L. Cohen, *Phys. Scr.* **T1**, 5 (1982). An energy cutoff of $11.5 R_y$ is used in the plane wave expansion, and a grid of up to 252 sampling \mathbf{k} points in the irreducible Brillouin zone is used for summations over the Brillouin zone.
- ¹⁰F. D. Murnaghan, *Proc. Nat. Acad. Sci. (USA)* **30**, 244 (1944).
- ¹¹P. K. Lam, M. M. Dacorogna, and M. L. Cohen, *Phys. Rev. B* **34**, 5065 (1986).
- ¹²W. L. McMillan, *Phys. Rev.* **167**, 331 (1968).
- ¹³P. K. Lam and M. L. Cohen, *Phys. Rev. B* **27**, 5986 (1983).
- ¹⁴M. M. Dacorogna, M. L. Cohen, and P. K. Lam, *Phys. Rev. Lett.* **55**, 837 (1985).
- ¹⁵K. H. Bennemann and J. W. Garland, in *Superconductivity in d- and f-Band Metals*, AIP Conf. Proc. No. 4, edited by B. H. Douglass (AIP, New York, 1972), p. 103.